Available online at www.sciencedirect.com

ScienceDirect

Physics Procedia 69 (2015) 252 – 257

Physics Procedia

10 World Conference on Neutron Radiography 5-10 October 2014

Limited-view Neutron CT Reconstruction with Sample Boundary

Hu Wang, Yubin Zou*, Yuanrong Lu, Zhiyu Guo

State Key Laboratory of Nuclear Physics and Technology, Peking University,
Beijing 100871, China

Abstract

Reconstruction of limited-view CT is an ill-posed inversion problem. In order to suppress the artefacts and improve the image quality, it has been proved to be a good method to incorporate some *a priori* information of the sample (refers to as constraint in this paper) to the iterative process. In this paper, sample boundary is considered as a constraint and SART algorithm is chosen to test the performance of the constraint. Reconstructions from different number of projections of the famous Shepp-Logan head phantom with different levels of noise were simulated; projection data of a spark plug was acquired on the cold neutron CT platform of China Advanced Research Reactor (CARR) and the spark plug was reconstructed as well. Both the simulation and experimental results show that SART algorithm with sample boundary constraint leads to remarkable improvement of image quality and convergence speed for limited-view CT reconstruction when the noise level of projection data is less than 5%.

Selection and peer-review under responsibility of Paul Scherrer Institut

Keywords: Neutron CT; Limited-view; SART; Sample boundary constraint

1. Introduction

With sufficient projection views, the attenuation coefficient matrix of the sample can be reconstructed with the filtered back-projection (FBP) algorithm fast and precisely; however, in many practical situations, such as industrial non-destructive testing[1], the number of projections is limited by the practical constraints. Iterative algorithms have advantages over FBP algorithm when the projection data is noisy and limited, but when only a few (ten or less) projections are available, severe streak artefacts still exist in the reconstructed image. The research of streak artefact suppression is reported in many papers. Some authors came up with tomogram post-processing[2]

* Corresponding author. Tel.: +86-010-62767895; fax: +86-010-62751875.
E-mail address: zouyubin@pku.edu.cn

Selection and peer-review under responsibility of Paul Scherrer Institut
doi:10.1016/j.phpro.2015.07.035

and projection pre-processing[3]. Some others[4] proposed that a certain kind of *a priori* information can be exploited to improve the quality of the constructed image, such as the non-negative constraint which based on the fact that the attenuation coefficient of the sample cannot be negative. In other cases, the composition of materials in the sample is known, and the maximum and minimum attenuation coefficient constraint is used [4]. Recently, the exact boundary of the sample can be precisely acquired with the 3D boundary scanning technique, which has the potential to provide a stricter constraint to the ill-posed problem. To assess the performance of the sample boundary constraint, numeric simulation and neutron CT-based experimental work were tested.

2. Method

Algebraic reconstruction technique (ART) was employed firstly by Hounsfield in his pioneering work on computed tomography[5]. It is based on a representation of the projection line integrals as ray-sums, which has been demonstrated that it can be employed advantageously in CT reconstruction from limited-view projections[6]. In the discrete setting, these ray integrals can be written as weighted sums over the pixels as:

$$\sum_{j=1}^{N} \omega_{ij}\, x_j = p_i, \qquad i = 1, 2, \dots M \tag{1}$$

The weighting factor ω_{ij} represents the intersection length of the *i*th ray through the *j*th pixel, which is determined by the projection geometry. p is the projection data obtained from experimental measurements. Thus the problem of reconstruction is to find the attenuation coefficient x through the known weighting factor ω and measurement p.

Simultaneous algebraic reconstruction technique (SART)[7] , an improved modification of ART, is a well-established iterative technique to solve the inversion problem. The sample boundary constraint is added to the process after each iteration. The iterative process can be written as:

$$\Delta x_j^n = \left(p_i - \sum_{j=1}^{N} \omega_{ij} \cdot\right) x_j^n \tag{2}$$

$$x_j^{n+1} = x_j^n + \lambda \cdot \frac{1}{\sum_{i=1}^{M} \omega_{ij}} \sum_{i=1}^{M} \frac{\omega_{ij}}{\sum_{j=1}^{N} \omega_{ij}} \Delta x_j^n \tag{3}$$

$$x_j^{n+1} = B\left(x_j^{n+1}\right) \tag{4}$$

where λ is the relaxing factor which can be chosen in the range from 0 to 2. For convenience, 1 is chosen in this paper. B is the operator of sample boundary constraint. Value of pixels out of the boundary will be set to zero after the operator.

The iteration process will stop after a set number of iterations. In order to evaluate the accuracy of the reconstructed image, Mean-Squared Error (MSE) [8]is taken into account.
The definition of MSE is:

$$MSE = \frac{1}{N} \sum_{j=1}^{N} \left(x_j^* - x_j\right)^2 \tag{5}$$

where x_j and x_j^* refer to the real and reconstructed pixel value of the image respectively.

As MSE is an absolute difference between the real image and the reconstructed image, the accuracy of the reconstruction cannot be clearly judged by this value. Here, Normalized Root MSE is employed, which is written as:

$$\mathrm{NRMSE} = \left[\frac{\sum_{j=1}^{N}\left(x_j^* - x_j\right)^2}{\sum_{j=1}^{N}\left(x_j - \bar{x}_j\right)^2}\right]^{\frac{1}{2}} \tag{6}$$

where $\bar{x}$ represents the mean value of all pixels in the real image. The value of NRMSE equals zero when the reconstructed image is totally the same as the real image. Generally, the smaller the NRMSE is, the better the image quality is.

3. Simulation results

In this section, the performance of the sample boundary-based SART algorithm is tested by numeric simulation. Projection data is generated from the high-contrast Shepp-Logan head phantom discretized on a 256×256 pixel grid as shown in Fig.1. Different levels of Poisson noise are added to the projection data to evaluate noise suppression performance of the algorithm. As for the simulation results presented here, only parallel beam configuration is considered. Comparison between rough boundary (mask1 as shown in Fig1.b) constraint and sample boundary (mask as shown in Fig1.c) constraint is tested as well.

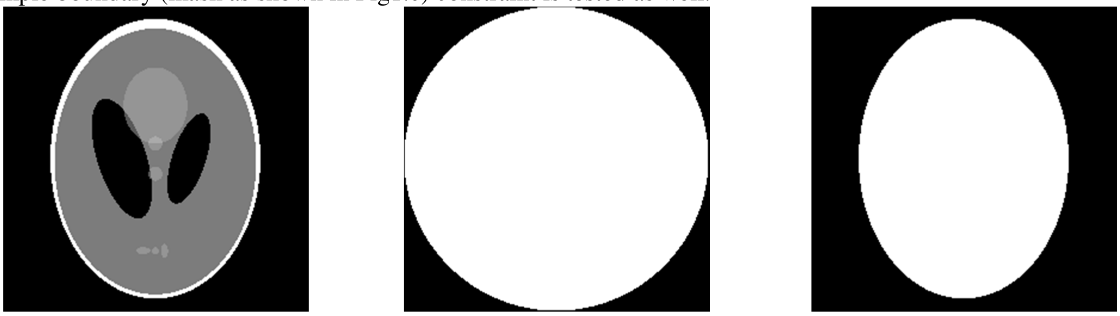

(a) (b) (c)

Fig.1.(a). Shepp-Logan head phantom ; (b) Rough boundary mask1; (c) Sample boundary mask

Fig.2 represents NRMSE of images reconstructed from 10 uniformly sampled views in the range of 0-180° with different Poisson noise level. It is obvious that when the noise level is less than 5%, the image quality reconstructed with sample boundary constraint (mask) is better than that with rough boundary constraint (mask1) and that without boundary constraint. In addition, the convergence speed of the sample boundary-based algorithm is faster than that of the other two.

4. Experimental results

Neutron CT projection data of a spark plug was acquired on the cold neutron imaging platform of China Advanced Research Reactor (CARR). Neutron flux at the sample position is in the magnitude of $10^7 cm^{-2}s^{-1}$.

Projections from 180 uniformly sampled views were taken in the range of 0-180° . Five images were taken at each single angle with total exposure time of ten seconds. A neutron image of the spark plug is shown in Fig.3. To illustrate the performance of the sample boundary-based SART algorithm, two slices of the spark plug are reconstructed.

Fig. 4 shows the reconstructed images of the chosen slices. The streak noise in the images reconstructed with the sample boundary constraint is suppressed more obviously.

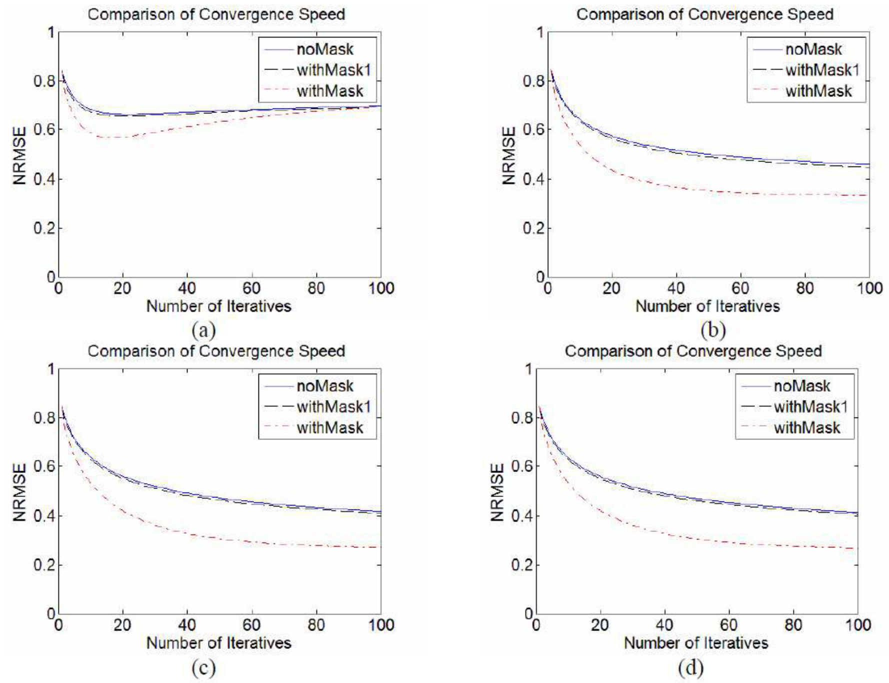

Fig.2. RMSE of image reconstructed from 10 uniformly sampled views in the range of 180 degrees with different noise level (a) 10% Poisson noise (b) 3.2% Poisson noise (c) 0.5% Poisson noise (d) clean

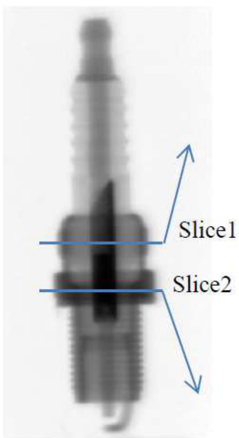

Fig.3. Neutron Image of the Spark plug

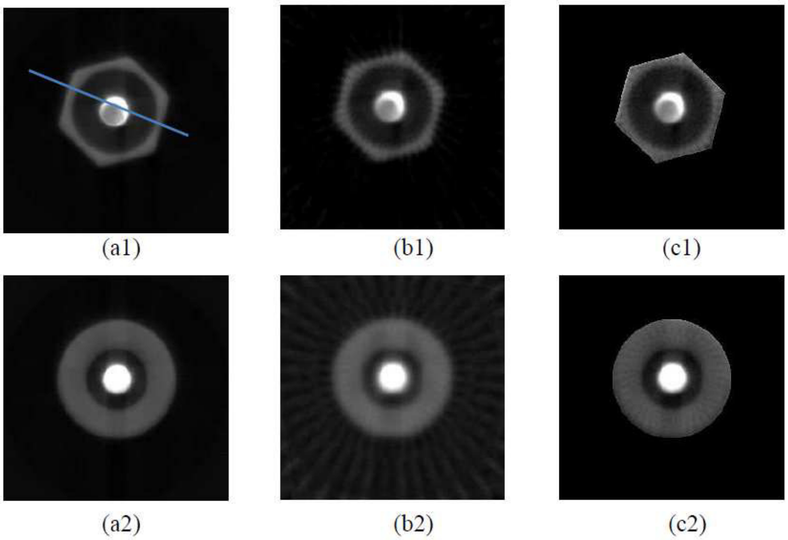

Fig.4.Reconstructions of two slices of the spark plug. The display window of grayscale is [0,0.04], [0,0.05] for slice 1 and slice 2 respectively (a) reconstructed image with FBP aglorithm from 180 projections (b) reconstructed image with SART aglotithm from 20 projections uniformly sampled in the range of 0-180° (c)reconstructed image with the sample boundary-based SART aglotithm from 20 projections uniformly sampled in the range of 0-180° .

For quantitative analysis, the intensity profile along the blue line in Fig4. (a1) are shown in Fig.5. The red dotted line is the profile of the image reconstructed from 180 views, which can be treated as the best estimation of the real distribution in this experiment. In the image reconstructed from 10 views and 20 views, the attenuation coefficients in the inner part are closer to the 180 views reconstruction when sample boundary constraint is used. However, because the intensity outside the sample boundary is set to zero by the boundary constraint, the layer inside the boundary becomes much more intense to compensate the blurred intensity which actually should exist outside the boundary.

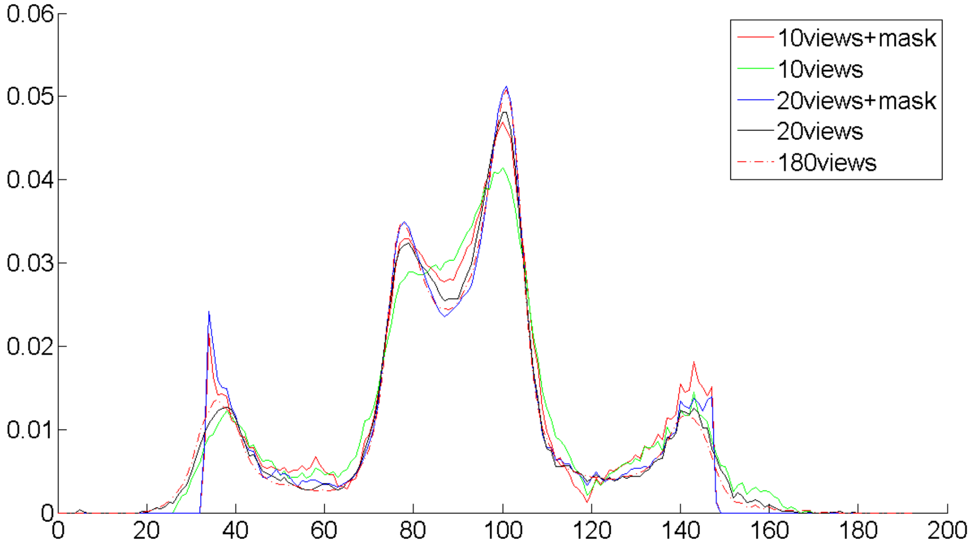

(a)

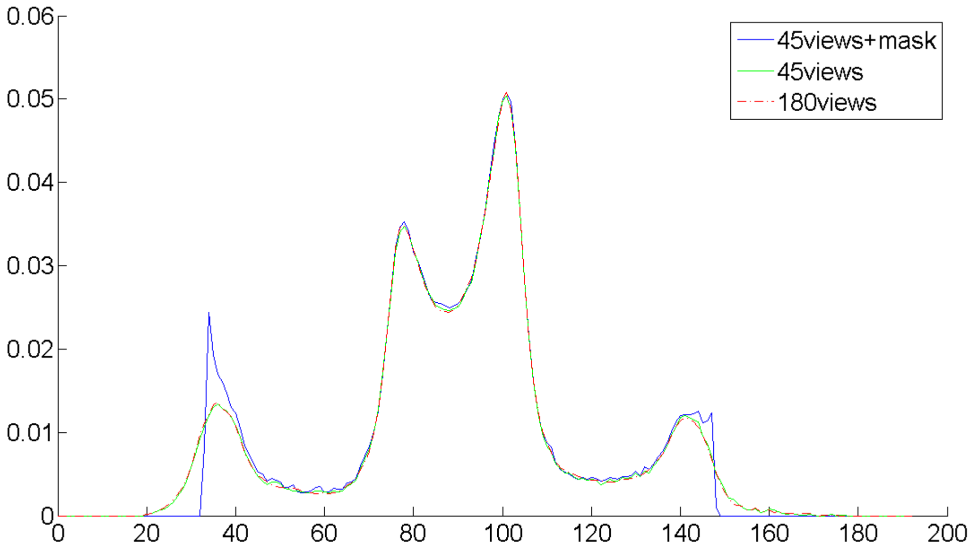

(b)

Fig.5. Comparison of the grayscale on profiles between images reconstructed from different views with and without boundary constraint

For reconstruction from 45 views, no striking difference is observed in the inner part. One possible reason is that the grey value outside the sample boundary is already negligible after sufficient number of iterations even without the boundary constraint for sufficient projection views like 45 or more. It is reasonable because the value outside the sample boundary will be as close as zero for infinite projection views, which means the boundary constraint helps little to improve the image quality in this condition. Nevertheless, the capability to accelerate the convergence speed of the boundary constraint still exists.

5. Conclusion

We have proposed a sample boundary-based iterative approach. SART algorithm is chosen to test the performance of the sample boundary constraint. Both numeric simulation and experiment show that for limited-view CT construction, like 10 views or 20 views, and with noise level of projection data less than 5%, the quality of the reconstructed image was improved with the sample boundary constraint. The convergence speed has improved as well. While for reconstruction with more views like 45 views in the situation of this work, the sample boundary constraint helps little for improving the image quality, which shows the limitation of the boundary constraint.

The sample boundary constraint also brings a higher intensity artefact inside the boundary. A constraint boundary slightly larger than the real geometry boundary may eliminate this effect, which will be studied in the coming work.

Acknowledgements

This work was supported by National Basic Research Program of China under grant no. 2010CB833106. We gratefully acknowledge the helpful support from the staff of China Advanced Research Reactor (CARR).

References

[1] Boyd J E. Limited-angle computed tomography for sandwich structures using data fusion[J]. journal of Nondestructive Evaluation, 1995, 14(2): 61-76.
[2] Henrich G. A simple computational method for reducing streak artifacts in CT images[J]. Computerized tomography, 1980, 4(1): 67-71.
[3] Morin R L, Raeside D E. A pattern recognition method for the removal of streaking artifact in computed tomography[J]. Radiology, 1981, 141(1): 229-233.
[4] Medoff B, Brody W R, Macovski A. The use of a priori information in image reconstruction from limited data[C]//Acoustics, Speech, and Signal Processing, IEEE International Conference on ICASSP'83. IEEE, 1983, 8: 131-134.
[5] C. N. Hounsfeld. "A method of and apparatus for examination of a body by radiation such as X or Gamma radiation." Patent Specification 1283915, London, 1968.
[6] Andersen A H. Algebraic reconstruction in CT from limited views[J]. Medical Imaging, IEEE Transactions on, 1989, 8(1): 50-55.
[7] Andersen A H. Algebraic reconstruction in CT from limited views[J]. Medical Imaging, IEEE Transactions on, 1989, 8(1): 50-55.
[8] Landi G, Piccolomini E L. An efficient method for nonnegatively constrained Total Variation-based denoising of medical images corrupted by Poisson noise[J]. Computerized Medical Imaging and Graphics, 2012, 36(1): 38-46.